The Influence of the Andes on Cutoff Lows: A Modeling Study*

RENÉ D. GARREAUD AND HUMBERTO A. FUENZALIDA

Department of Geophysics, Universidad de Chile, Santiago, Chile

(Manuscript received 1 February 2006, in final form 1 June 2006)

ABSTRACT

A cutoff low (COL) pressure system that occurred in March 2005 (late austral summer) over the subtropical southeast Pacific is examined by means of numerical simulations using the Weather and Research Forecasting (WRF) model. The episode exhibited typical features of COLs in this region, including its formation from an elongated northwest–southeast extratropical trough and subsequent intensification off the west coast of South America. During the developing stage, the cyclonic circulation did not extend into the lower troposphere and only upper-level, nonprecipitating clouds were observed at and around the system. When the COL reached the continent it produced moderate but unseasonal rainfall along the semiarid western slope of the Andes cordillera [summit level at ~5000 m above sea level (ASL)] at the same time that the system experienced a rapid decay. The control simulation used full physics, full topography, and a single domain (54-km grid spacing) laterally forced by atmospheric reanalysis. Model results are in general agreement with upper-air, surface, and satellite observations, and allow a detailed description of the three-dimensional structure of the COL, as well as an evaluation of the vorticity and temperature budgets. A quasi-stationary, amplifying warm ridge over the South Pacific appears as the key precursor feature, in agreement with studies elsewhere. Once the COL formed, it drifted eastward mostly driven by vorticity advection induced by its own circulation, and there was close balance between vertical and horizontal temperature advection near its center. The jet streak along the COL's periphery migrated from upstream of the COL axis, during the developing stage, to downstream later on. Four sensitivity experiments—reducing/removing topography, suppressing hydrometeors, and using an enlarged domain—were performed to assess the influence of the Andes, the importance of latent heat release, and the effect of the boundary conditions. Comparison among the control and sensitivity runs indicates that the COL formation occurs regardless of the presence of the Andes, and COL dissipation is mainly due to latent heat released in the deep clouds that form over the mountainous terrain. Nevertheless, the Andes cordillera delayed the COL demise by blocking the inflow of warm, moist air from the interior of the continent that otherwise would initiate deep convection in the region of ascending motion downstream of the COL.

1. Introduction

Cutoff lows (COLs) are upper-level, low pressure centers formed on the equatorward side of the maximum westerly flow in the polar or subtropical jet stream. They develop from a trough that experiences a marked tilting and subsequent breaking off, leaving a pool of cold air and cyclonic circulation detached from the extratropical wave (e.g., Palmén 1949). Once a COL has formed, it exhibits a quasi-barotropic structure throughout the mid- and upper troposphere, a horizontal scale of a few hundred kilometers, and can persist for several days before being destroyed by processes such as diabatic heating or friction, or moving back into high latitudes (Hoskins et al. 1985). On an isentropic surface near the tropopause, COLs are revealed as isolated centers of high potential cyclonic vorticity. Thus, their formation and intensification has often been described within the potential vorticity framework (e.g., Hoskins et al. 1985; Bell and Bosart 1993).

Because in a COL the core of the cold air is located in the mid- and upper troposphere, the air column underneath can become statically unstable, provided a favorable surface condition exists (e.g., COLs moving over a warm ocean). Indeed, deep convection and se-

* Supplemental information related to this paper is available at the Journals Online Web site: http://dx.doi.org/10.1175/MWR3350.s1.

Corresponding author address: Dr. René Garreaud, Departamento de Geofísica, Universidad de Chile, Blanco Encalada 2002, Santiago, Chile.
E-mail: rgarreau@dgf.uchile.cl

DOI: 10.1175/MWR3350.1

vere weather associated with COLs have been reported in southern Europe (Nieto et al. 2005), eastern Australia (e.g., McInnes and Hess 1992), and eastern South America (Miky-Funatsu et al. 2004). COLs can also bring strong winds, heavy snowfall, and unusual cold conditions to high-elevation regions (e.g., Vuille and Ammann 1997). Furthermore, strong vertical motion around the COL leads to tropopause folding and tropopause erosion due to deep convection and turbulent mixing, thus increasing stratosphere–troposphere exchange (STE) of trace gases (Hoskins et al. 1985; Price and Vaughan 1993). For instance, episodes of high-tropospheric ozone concentration in subtropical areas of both hemispheres have been linked with COLs (e.g., Kentarchos et al. 2000; Rondanelli et al. 2002). The previous factors, added to the often erratic displacement of COLs, make their forecast a particularly challenging problem.

The spatial and seasonal distribution of COLs has been documented in climatological studies for the Northern (Kentarchos and Davies 1998; Smith et al. 2002; Nieto et al. 2005) and Southern Hemisphere (Fuenzalida et al. 2005). In both, COLs tend to be more frequent at subtropical latitudes over the continents and adjacent oceans, while fewer COLs are found on the midlatitude storm tracks. Northern Hemisphere COLs are more frequent in summer than in winter in all three regions where they prevail (North America, southern Europe, and Southeast Asia). In contrast, COL frequency over the African and South American regions is maximum in austral winter, while COL frequency over the Australian region remains nearly invariant during the year.

A closer inspection of the spatial distribution of COLs in the SH reveals a tendency for a net generation of COLs on the upwind (western) side of the continents and a net destruction on the lee side (Fuenzalida et al. 2005, their Fig. 1). This feature is particularly well defined near South America, where a prominent region of COL genesis is observed off the west coast, while few COLs are generated over the continent farther east. Moreover, only a fourth of the COLs formed over the adjacent Pacific can be traced inland; synoptic experience indicates that most of the COLs in this region begin to develop deep convection and rainfall in their eastern flank as they approach the Andes cordillera and subsequently "fill up" as they cross the mountains. The Andes runs continuously and very close to the coast, rising up to 5000 m ASL at subtropical latitudes and up to 1500 m ASL farther south. Thus, one may hypothesize that the presence of the Andes (i) favors the genesis of COLs over the eastern Pacific by blocking the tropospheric flow at low- and midlevels, and (ii) contributes to the COL demise by initiating or enhancing deep convection.

Unfortunately, the upper-air network over the southeast Pacific and South America is not dense enough to document the three-dimensional structure and evolution of the COLs, especially their interaction with the Andes. Similarly, the horizontal resolution of the available global atmospheric reanalysis is marginal to resolve the COL structure [e.g., $2.5° \times 2.5°$ latitude–longitude for the National Centers for Environmental Prediction–National Center for Atmospheric Research (NCEP–NCAR) reanalysis]. Aiming at a better description and diagnosis of COLs in western South America, in this work we performed an 8-day numerical simulation of a typical case that occurred in March 2005. In this study we use the Weather and Research Forecasting (WRF) model (Skamarock et al. 2005), on a single domain with a horizontal grid spacing of 54 km (see details in section 2). The model results were validated whenever possible with observations, and allow us a synoptic-scale description of the episode (section 3). Furthermore, the COL dynamics is studied using several diagnoses of the model results, including a term-by-term evaluation of the thermodynamic and vorticity equations (section 4). To test our hypothesis on the role of the Andes upon the COL life cycle, four additional "sensitivity experiments" were performed using WRF: a simulation in which the terrain was reduced by a factor of 0.2 everywhere, a dry simulation, a simulation using a larger domain, and a simulation in which the terrain elevation was reduced by a factor of 0.0 everywhere in the extended domain (section 5). While in this work we analyze one single episode near the Andes cordillera, some of our conclusions (section 6) might be generally applicable to the effect of the topography upon COLs elsewhere.

2. Model setup and experiment details

To obtain a comprehensive three-dimensional description of a COL, a numerical simulation of a typical episode was performed using WRF version 2. This simulation is referred to as control (CTR), since it includes the full model physics and a realistic topography. The WRF is an area-limited, fully compressible, nonhydrostatic numerical model formulated in Arakawa C-grid staggering horizontal grid and a terrain-following hydrostatic pressure vertical coordinate, as described in detail in Skamarock et al. (2005). The model physics has five categories, each containing several options; the parameterizations used in CTR are listed in Table 1. Of particular relevance is the use of the WRF Single-Moment 3-Class (WSM3) scheme for

TABLE 1. Physical parameterizations used in the WRF for the control simulation.

Processes	Scheme	Reference
Cumulus convection	Kain–Fritsch	Kain and Fritsch (1993)
PBL turbulence	Gayno–Seaman	Gayno (1994)
Radiation	Cloud radiation	Hong et al. (2004)
Moisture	Simple ice	Hong et al. (2004)
Ground temperature	Force–restore	Blackadar (1979)

microphysics, following Hong et al. (2004). This is a so-called simple ice scheme that includes water vapor, cloud water–ice, and rain–snow.

The control simulation features a single domain, covering subtropical and southern South America and the southeast Pacific (15°–60°S, 97°–55°W), with a horizontal grid spacing of 54 km and 29 vertical levels. Initial conditions and time-dependent lateral boundary conditions were obtained by interpolating NCEP–NCAR reanalysis every 6 h (Kalnay et al. 1996). Surface boundary conditions (skin temperature) were also taken from NCEP–NCAR reanalysis (fixed at initial time). The observed COL persisted from 9 to 12 March 2005. To capture the full COL life cycle, the simulation spans from 0000 UTC 6 March to 0000 UTC 14 March 2005.

To test our hypothesis on the effect of the Andes upon a COL, four additional "sensitivity" WRF simulations were carried out. They had the same initialization time and duration (8 days) as the control run, and they were also forced by NCEP–NCAR reanalysis. The specific details of each simulation are as follows:

- Reduced Topography (RTopo): In this simulation the terrain elevation was reduced by a factor of 0.2 everywhere. It uses the same domain, resolution, and physic options as CTR.
- Dry (Dry): In this simulation WRF was run with no water vapor or hydrometeors. It uses the same domain, resolution, and other physic options as CTR.
- Extended Domain (ED): In this simulation all the lateral boundaries were expanded outward with respect to those in CTR; in particular, the western boundary was placed 35° to the west that in the control simulation. Thus, the extended domain is about twice as large as the CTR domain, but the resolution was set to 108 km. The ED uses the same physics options as CTR.
- Extended Domain No-Topo (EDNT): In this simulation we use the extended domain (5°–60°S, 133°–50°W) and coarse resolution (108 km), but the terrain elevation was reduced by a factor of 0.0 everywhere. It uses the same physic options as CTR.

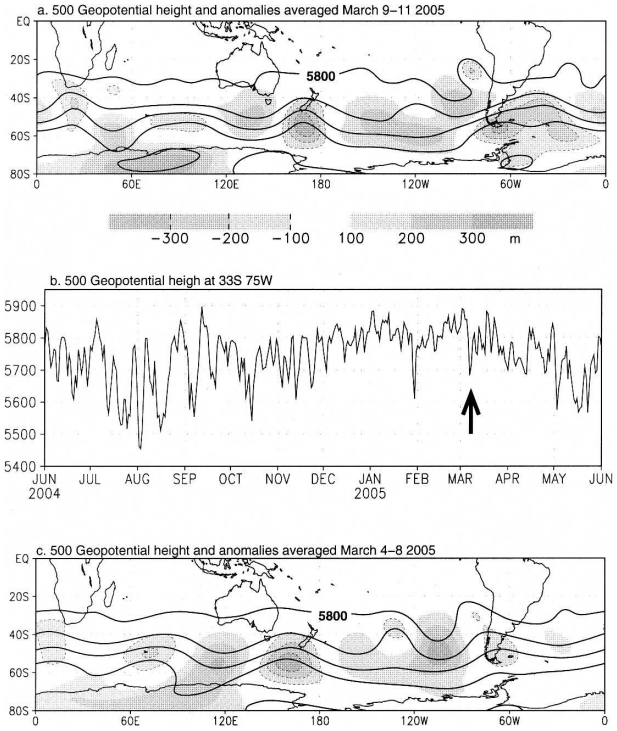

FIG. 1. (a) 500-hPa geopotential height averaged between 9 and 11 Mar 2005. The contour interval is 100 m. Shading indicates departures from the climatology according to the scale at the bottom (dashed lines indicate negative anomalies). (b) Daily values of 500-hPa geopotential height at 33°S, 75°W. The episode analyzed in this work is indicated by the arrow. (c) Same as in (a) but for 4–8 Mar 2005. Data source: NCEP–NCAR reanalysis.

3. Synoptic-scale structure

a. Large-scale context

The episode analyzed in this work took place between 9 and 11 March 2005 (late austral summer) and, as we show later, it exhibits many of the features that are often observed in western South America (e.g., Pizarro and Montecinos 2000). To place this episode in context, Fig. 1a shows the reanalysis 500-hPa geopotential height (Z_{500}) and geopotential height anomalies (departure from the monthly long-term mean) averaged during the episode. There are no closed geopotential contours in the average field (due in part to the specific contour drawn and the smoothing effect of the temporal average), but the midlevel depression is readily evident over the subtropical southeast Pacific. Grid points within this region experience a drop in Z_{500} down to about 5650 m during COL's passage (Fig. 1b), a very low value for the summer season. The area of negative Z_{500} anomalies at subtropical latitudes is, however, rather small compared with anomalies observed

in midlatitudes, emphasizing the subsynoptic scale of the COL.

Especially important is a broad area of positive anomalies extending from the south-central Pacific all the way to southern South America, which was in place several days before the COL formation (Fig. 1c). Thus, the major large-scale feature prior to the episode was an intense, quasi-stationary ridge over the south Pacific just upstream of the cyclogenesis region. Similar precursor ridges were found in case studies of COLs over the eastern United States (Bell and Bosart 1993) and over eastern South America (Mishra et al. 2001).

b. Horizontal circulation

Model-derived (CTR simulation) maps of 300-hPa geopotential height and wind speed, from 7 to 12 March, are shown in Fig. 2. Early in the simulation, a deep trough dominated the circulation over most of South America, well extended into subtropical latitudes (Fig. 2a). By 8 March (Fig. 2b) the midlatitude portion of the trough moved into the South Atlantic while its subtropical portion remained to the west of the Andes, increasing the horizontal tilt of the trough axis. The upstream ridge amplified during the preceding 24 h, tightening the horizontal temperature gradient over the southeast Pacific (not shown) and thus strengthening the westerlies at about 50°S. Furthermore, a southeasterly jet formed between the upstream ridge and the trough, with wind speeds $\sim$15 m s^{-1} higher than the northwesterly jet immediately downstream of the trough. This asymmetric wind field is typical of pre-COL environments (Bell and Keyser 1993), producing advection of cyclonic vorticity toward the trough base and the subsequent trough amplification (Keyser and Shapiro 1986).

Geopotential contours began to close at about 0600 UTC 9 March 2005 over the subtropical southeast Pacific while the parent trough continued moving eastward, so that by 1800 UTC of that day the cyclone was fully segregated (Fig. 2c). One day later (Fig. 2d) the parent trough had left the model domain, the COL deepened and became more circular, and the circulation at midlatitude was dominated by a broad ridge. The COL reached its maximum strength around 1800 UTC 11 March 2005 (Fig. 2e), with its center at about 1000 km off the coast of Chile. By 1800 UTC 12 March 2005 (Fig. 2f) the system was over central Argentina, but its size and strength had reduced significantly, so only a trough can be identified with the contour interval used in the previous maps. In the last 24 h of the simulation, the trough weakened as it moved near the Atlantic seaboard. It should be noted, however, that roughly half of upper-level troughs experience a marked deepening accompanied with rapid surface cyclogenesis over the eastern side of the continent (e.g., Hoskins and Hodges 2005). (The causes behind the different evolution of COLs as they cross the Andes are beyond the scope of this paper, but they deserves further investigation.)

The evolution of the jet streak during the COL's life cycle strongly resembles the stages described in Keyser and Shapiro (1986). Initially (Fig. 2b) the main streak is upstream of the inflection point while later on (Figs. 2d,e) it has move to the downstream side. The intermediate stage with the streak over the trough–COL axis was not obtained in spite of a revision at a 2-h interval, but this is to be expected due to the small scale of the system. As the streak approaches the inflection point, the trajectory curvature becomes so large that the gradient wind must decrease to a point that the speed maximum becomes unnoticed. Afterward, the speed increases as the curvature becomes smaller and the streak is again well defined downstream of the COL.

There are no upper-level observations off the Chilean coast to validate the model results near the COL center during its developing stage. Yet, radiosonde data from Santo Domingo, Chile, a coastal station at 33°S, and Aircraft Communications Addressing Reporting System (ACARS) data, provide a good opportunity for model validation. Figure 3 shows the time evolution of the air temperature at 850, 500, and 200 hPa, from which a good correspondence between observations and model results is evident ($r > 0.75$ in all levels). In particular, the model did capture the amplitude, timing, and vertical extent of the two cooling events at midlevel during the simulation period: the first ending at 1200 UTC 8 March 2005, and the second ending at 1200 UTC 12 March 2005. The first cooling was associated with the arrival of the extratropical trough to the Chilean coast, extended well into the lower troposphere, and produced a moderate descent of the tropopause as evidenced in the warming at 200 hPa. The subsequent midlevel warming occurred as the trough increased its northwest–southeast tilt, thus retreating from the continent at subtropical latitudes. The second, COL-related cooling and subsequent warming was very sharp (10°C day^{-1}) in the middle troposphere, but its magnitude decreased significantly at lower levels. Simultaneously, there was a marked warming at 200 hPa associated with a pronounced depression of the tropopause.

Hourly surface observations, although rather indirectly linked to the COL, provide additional data to validate the model. Figure 4 shows several variables recorded in Santiago at the Andes foothills (33°S, 72°W, 530 m ASL) together with the model results in-

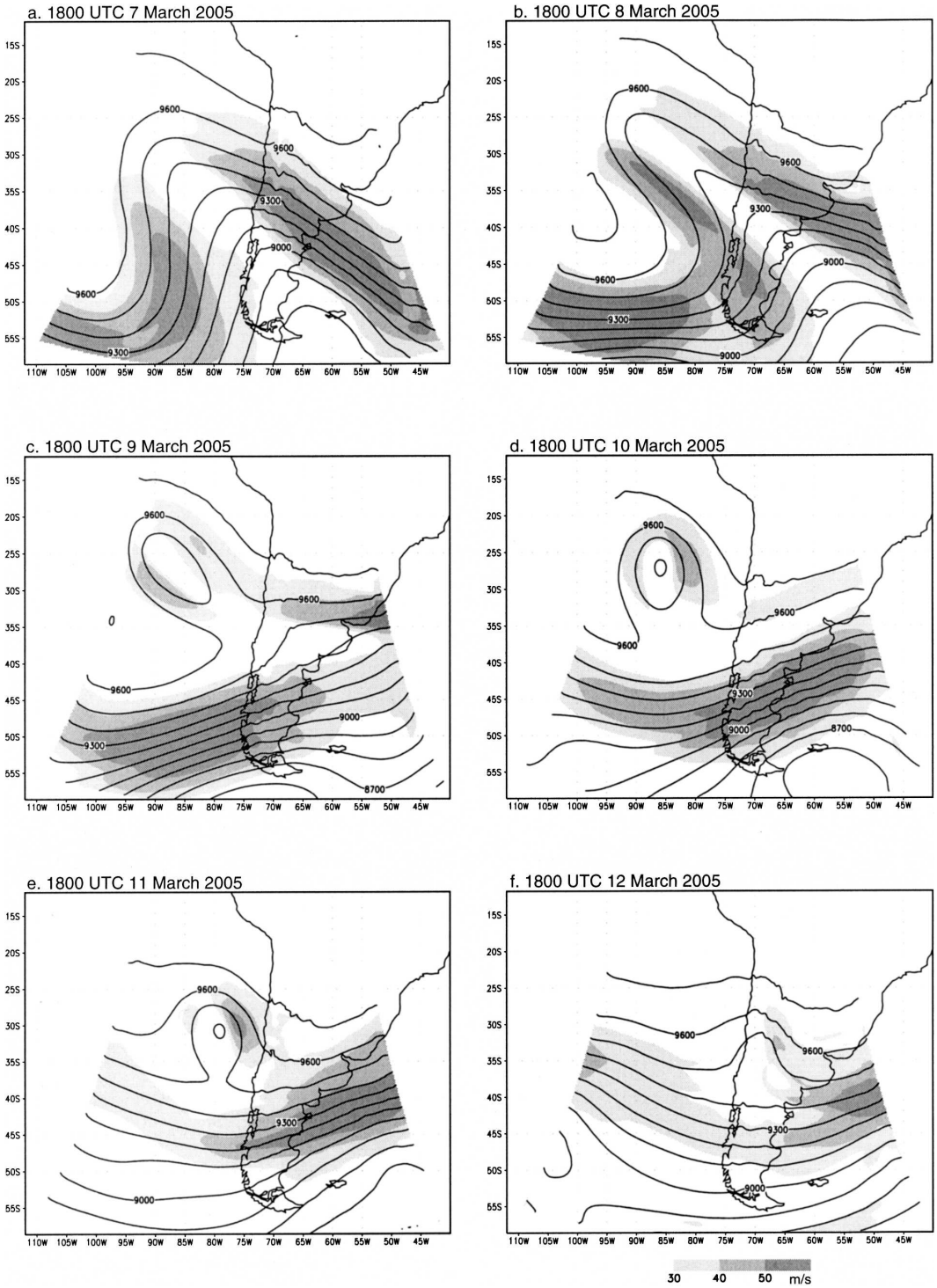

FIG. 2. Model geopotential height [contour interval (CI) 100 m] and wind speed (shaded, scale at the bottom) at 300 hPa, at 1800 UTC (a)–(f) from 7 to 12 Mar 2005 (date and time indicated).

terpolated to that point. A good correspondence is observed in surface pressure, except for a 6-h difference in the timing of the minimum during the COL passage. The comparison between modeled and observed surface air temperature is less favorable, although the model was still able to replicate the two cooling events. The model accurately reproduced the amount and timing of the rainfall that fell over Santiago on the night of

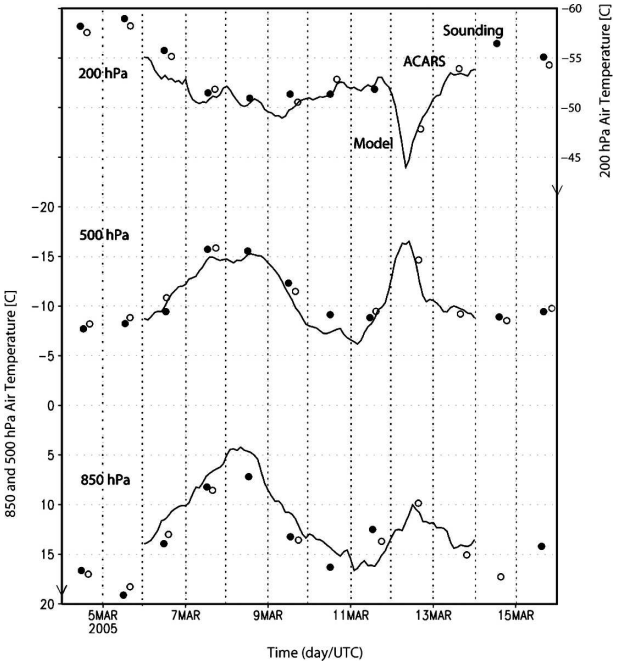

FIG. 3. Time series of the air temperature at 850, 500, and 200 hPa over central Chile. Model results at 33°S, 72°W (solid line). Radiosonde data from Santo Domingo (33.4°S, 71.7°W) (solid circles). Soundings are performed at 1200 UTC. ACARS data from commercial aircraft departing/arriving at Santiago International Airport (33.2°S, 72.5°W) (open circles).

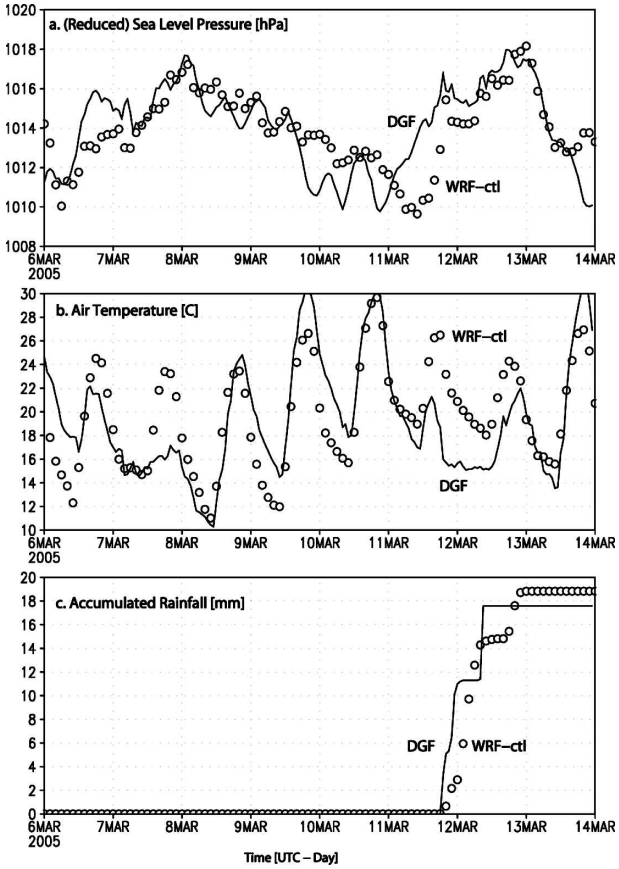

FIG. 4. Observations (solid lines) and model results (open circles) of several surface variables in Santiago (33°S, 72°W, 530 m ASL). Observations from an automatic weather stations with a 15-min sampling interval. Model results bilinearly interpolated to Santiago. (a) Surface pressure reduced to sea level pressure, (b) 2-m air temperature, and (c) accumulated rainfall.

12 March, when the COL was crossing the Andes [20 mm $(12\ \text{h})^{-1}$ is a significant rainfall event for semiarid central Chile, even for winter standards, and it caused some major disruption in Santiago].

c. Vertical motion and cloudiness

Maps of vertical velocity and geopotential height at 400 hPa (w_{400} and Z_{400}, respectively) during the COL intensification stage and near the time of maximum intensity are shown in Fig. 5. In both cases, the most relevant feature is a couplet of vertical velocity, with subsidence on the western flank of the COL and ascent in the eastern flank. During the intensification period, the subsidence was much stronger and encompasses a much larger area than the ascent. By the time of the COL maximum intensity the ascending motion became more prominent. Later on, the ascent maintained its strength, even when the COL was decaying near the Andes, likely because of the contribution of the topographic uplift in the windward side of the mountains.

To further describe the vertical structure of the system, Fig. 6a shows a time–height diagram of w and θ for a point about 400 km off the coast of central Chile. The ascent before the passage of the COL's center extended from the lower troposphere well into the tropopause (700–150 hPa), with a maximum between 250 and 200 hPa. The subsidence after the passage of the COL was slightly stronger but occurred in a shallower layer (600–200 hPa), and maximized at lower levels (400–300 hPa). Figure 6b also shows w and θ but in a zonal cross section (longitude–height) along 31°S near the time of maximum COL strength. The vertical motion couplet is roughly symmetric with respect to the COL center. Cores of strong ($>20\ \text{cm s}^{-1}$) ascending motion are found in the midtroposphere both upstream, over, and downstream of the mountains, as well as strong downslope flow in the eastern slope of the Andes.

Model-derived cloud mixing ratio vertically averaged between 600 and 300 hPa (Q_C) is shown in Fig. 7 for several times. Regions covered by mid- and upper-level clouds were identified as contiguous grid boxes with $Q_C > 1 \times 10^{-5}\ \text{g kg}^{-1}$. These maps are complemented by vertical profiles of cloud mixing ratio for selected

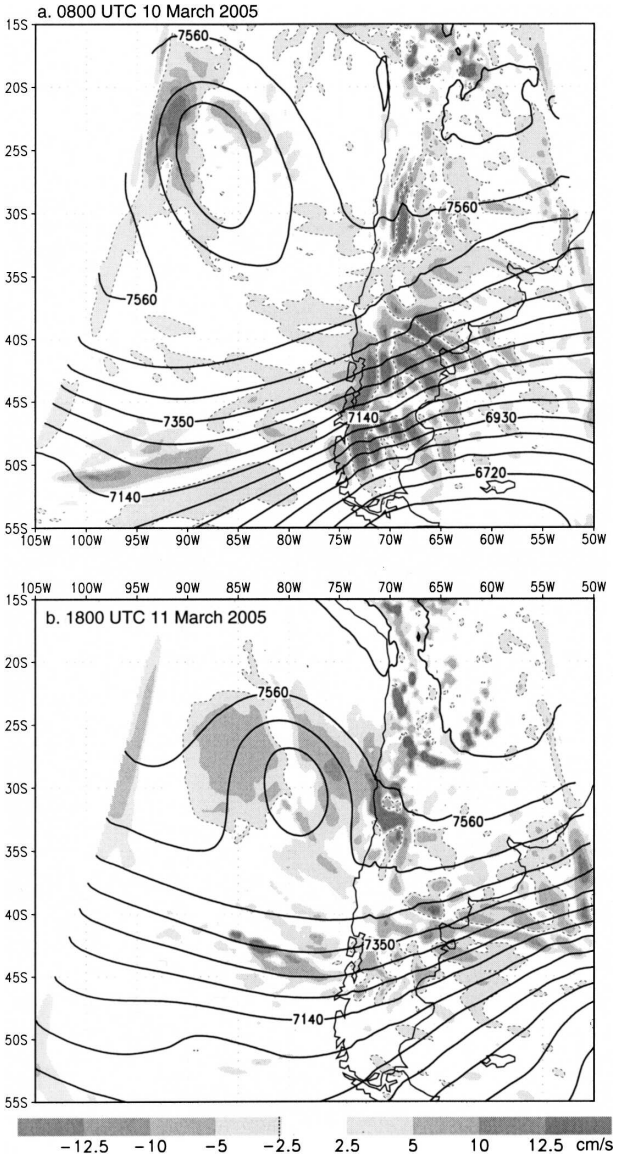

FIG. 5. (a) Model geopotential height (CI 70 m) and vertical velocity (shaded) at 400 hPa on 1600 UTC 10 Mar 2005. Dashed lines outline regions of downward motion ($w < 0$). (b) Same as in (a) but for 1600 UTC 11 Mar 2005.

points/dates (Fig. 8). Overall, during the intensification period (8–10 March 2005, Figs. 7a,b) there was little cloudiness at and around the COL; instead, a deep cloud band at midlatitudes moved rapidly eastward just downstream of the trough. A filament of high-level clouds extending from the midlatitude trough to the subtropical COL (the so-called streamer) was evident until 1800 UTC 9 March 2005.

During the first half of 11 March 2005, upper-level clouds developed at the COL's center, but they had little water content (Figs. 7c and 8a) and did not precipitate. At about 1800 UTC, a rapid cloud development took place along the western side of subtropical Andes, in the region of strong northwest flow downstream of the COL. This cloud band had high water content, encompassed the upper and midtroposphere, and produced 20–30 mm of rainfall over the mountainous terrain and the adjacent lowlands near the coast (Fig. 8b). The troposphere in this sector became slightly unstable (CAPE ~200 J kg^{-1}), a rather unusual condition in central Chile. Once the upper-level system moved to the east of the Andes, deep, thick clouds covered central and eastern Argentina, producing up to 50 mm of rainfall, mostly of convective nature (CAPE ~900 J kg^{-1}; Fig. 8c).

The model-derived cloud distribution is in general agreement with the actual distribution obtained from the *Geostationary Operational Environmental Satellite-12* (*GOES-12*) imagery (Fig. 9). In particular, the satellite images confirm the rapid development of the clouds over the Andes as the COL approached this region. Nevertheless, the actual cloud band was longer than the model one, extending continuously from the subtropical Andes into the southern flank of the COL. The sharp contrast in depth, liquid water content, and rainfall of the clouds near the center of the "oceanic" COL compared with those ahead of the system over the continent, were also in general agreement with rainfall-rate maps and vertical profiles of hydrometeors derived from the Tropical Rainfall Measuring Mission (TRMM) Microwave Imager (TMI) data (2A12 algorithm; not shown).

4. Model diagnosis

a. Segregation process

Although the segregation mechanism is not central to this article, some descriptive remarks are in order. Figure 10 shows the potential vorticity (PV) on the 340-K isentropic surface and the geopotential and wind fields on the 300-hPa isobaric surface at several times during the simulation, where the COL's segregation, intensification, and decay are readily evident. Previous to the COL formation, a relatively broad area of cyclonic PV extends along the axis of the parent trough from the midlatitude into the subtropics (Figs. 10a,b). Because the warm ridge over the South Pacific (to the west of the COL genesis region) has a meridional axis, the flow upstream of the trough is mostly southerly forming an acute angle with the trough axis and producing strong anticyclonic (positive) vorticity advection (AVA) into the trough axis at midlatitudes. In contrast, the downstream flow is nearly parallel to the trough axis and the cyclonic vorticity advection (CVA) is weaker. Strong

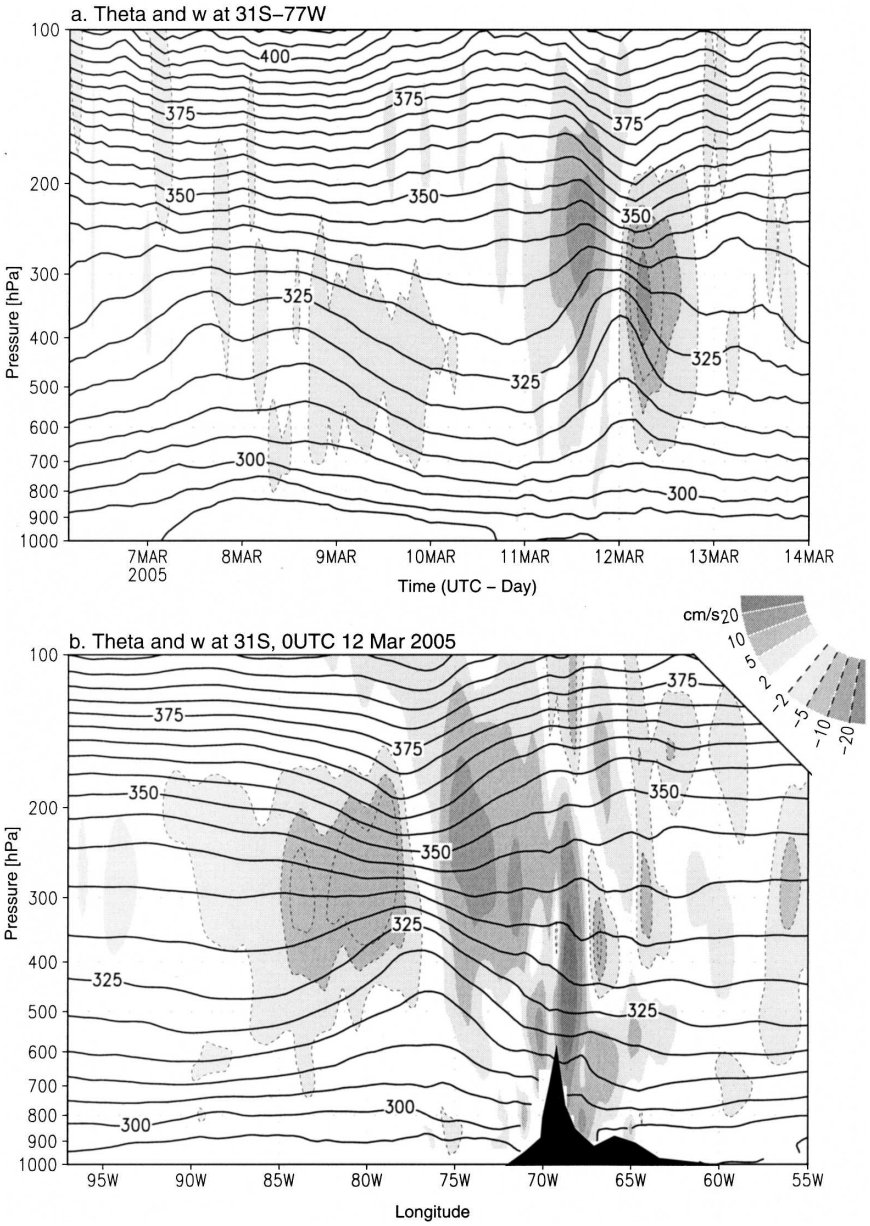

FIG. 6. (a) Time–pressure diagram of potential temperature (CI 5 K) and vertical velocity (shaded, scale at bottom) at 31°S, 77°W during the simulation period. Dashed lines outline regions of downward motion ($w < 0$). (b) Same as in (a) but for a zonal (longitude–pressure) section at 31°S on 0000 UTC 12 Mar 2005. The topographic profile at this latitude is indicated by the black area.

AVA upstream of the trough axis also leads to strong descent and adiabatic warming, acting in concert with horizontal warm advection at midlatitudes. Downstream of the trough, weak CVA goes along with weak (if any) ascent, so the cooling in that side is very small. Hence, from a dynamical and thermodynamical perspective, the initial asymmetry in the wind direction around the parent trough seems key in the cyclone segregation, because it strangles the northwest–southeast-elongated cold trough at midlatitudes near the coastline. Thus, the system segregated completely from 9 to 10 March 2005 (Fig. 10c). During the next two days the potential vorticity intensified reaching a maximum of −8 PVU near the COL center, the lowest value north of 55°S throughout the complete simulation (Fig. 10d). Later, when the COL warmed by the release of latent

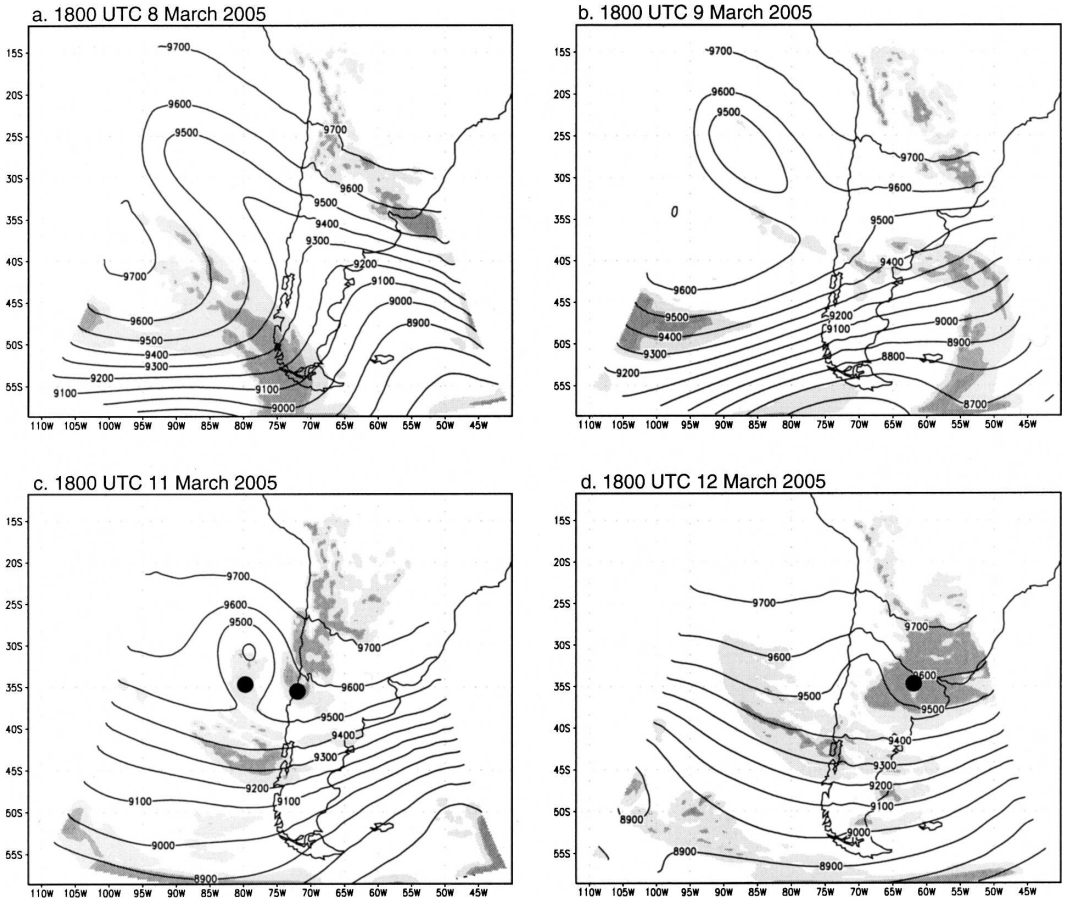

FIG. 7. Model geopotential height (CI 100 m) at 300 hPa and cloud mixing ratio integrated between 600 and 300 hPa [light shading >1 ($\times 10^{-5}$ g kg^{-1}), dark shading >10 ($\times 10^{-5}$ g kg^{-1})] at 1800 UTC (a) 8, (b) 9, (c) 11, and (d) 12 Mar 2005. Closed circles in (c) and (d) indicate position of vertical profiles shown in Fig. 8.

heat it became weaker and merged with its original source of an air mass after 12 March 2005 (Fig. 10e).

b. Vorticity and temperature budget

We now focus on the mature stage of the COL. The relative vorticity field at 300 hPa on 10 March 2005 (Fig. 11a), presented an ellipsoidal shape with values smaller than -20×10^{-5} s^{-1} over a ring spreading from 21° to 33°S. Such values correspond to rather large relative vorticities, 3–4 times the Coriolis parameter. Large shear vorticity dominates on the west and east flanks of the COL associated with the lateral jets, while curvature vorticity dominates on the northward and southward sections of the COL. In the ring northern half, the major axis of the COL separated two centers with maximum values of $\sim 80 \times 10^{-10}$ s^{-2} in the local variation of relative vorticity in the upwind and downwind flanks, respectively, consistent with an eastward drift of the system at about 10 m s^{-1} (Fig. 11a). In the full vorticity equation, the largest term is the horizontal advection of relative vorticity, which is negative over most of the COL periphery (Fig. 11b). This term is modified by vertical transport and horizontal divergence, with minor contributions from the tilting term, leading to the anticyclonic (cyclonic) tendencies at the upwind (downwind) side of the COL.

On the same day, 10 March 2005, at the 400-hPa level, the pattern of local temperature change was composed of slight warming (+0.5 K day^{-1}) in the northwestern fringe of the COL and cooling (−0.5 K day^{-1}) on the eastern side (Fig. 11c). Near the COL center tendencies are very small. Such a pattern corresponds to a small residue between relatively large horizontal and vertical temperature advection (~4 K day^{-1}). In particular, there is cold advection on the western side and warm advection on the eastern side of the COL (Fig. 11d), and similar but opposing contributions by vertical motion.

The secondary circulation obtained in the numerical simulation of the COL agrees in many aspects to that

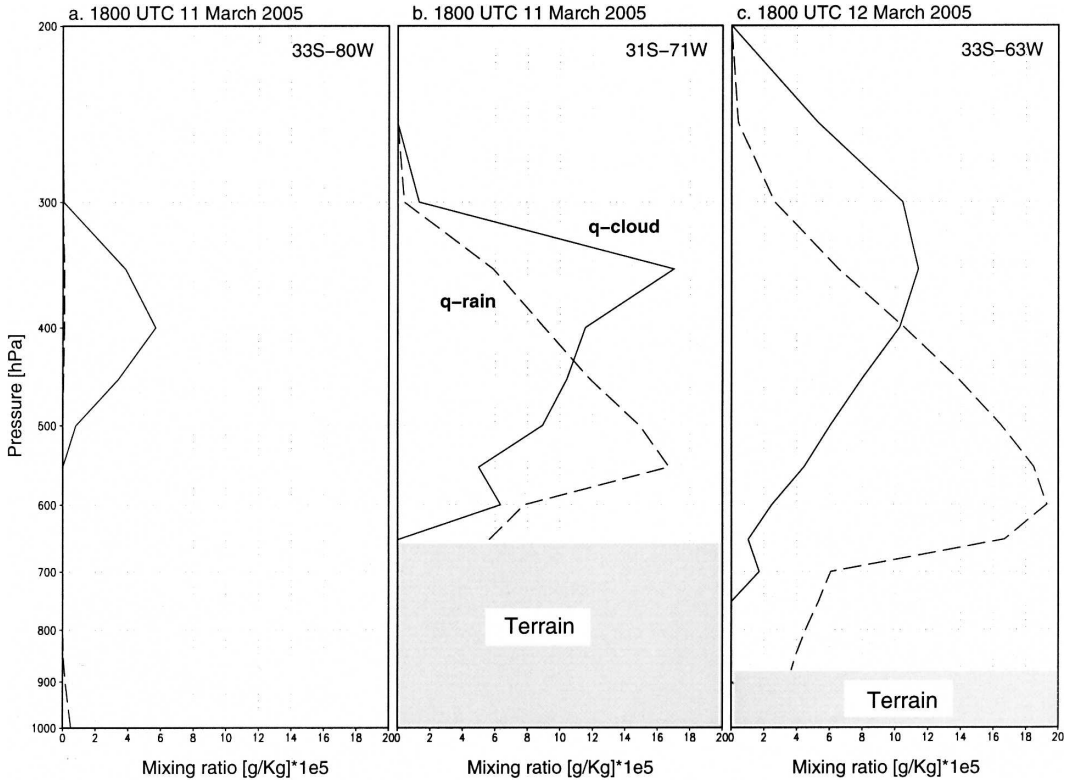

FIG. 8. Vertical profiles of cloud (solid line) and rain (dashed line) mixing ratios at (a) 33°S, 80°W on 1800 UTC 11 Mar 2005, (b) 31°S, 71°W on 1800 UTC 11 Mar 2005, and (c) 33°S, 63°W on 1800 UTC 12 Mar 2005 (see points/dates in Fig. 7).

described by Keyser and Shapiro (1986) in their review of upper-level frontal zones. In particular the mid- and upper-level vertical velocity in the warm air mass surrounding the COL closely follows their description, with downward motion (indirect circulation) upstream of the COL axis and upward motion (direct circulation) downstream (e.g., Fig. 5b).

5. Sensitivity experiments

While the previous diagnoses reveal the key processes responsible for the COL's intensification far from the Andes, their evaluation and interpretation becomes more difficult over the mountainous terrain, where the COL experiences its demise. Therefore, in this section we contrast the results from the sensitivity experiments to shed light on the role of the topography and diabatic warming on the COL life cycle. Figure 12 shows Z_{300} and T_{500} at two fixed times during the CTR, RTopo, and Dry simulations. Because the COL's center tracked almost zonally between 28° and 32°S, several aspects of its evolution can be conveniently described by time–longitude diagrams of different variables averaged in that range (hereafter identified as [var]) as shown in Figs. 13 and 14.

The first time shown in Fig. 12 (1200 UTC 10 March 2005, left panels) is representative of the COL intensification stage (as simulated in CTR). The overall pattern—subtropical COL/midlatitude ridge—is similar in all the simulations. In particular RTopo and Dry produce a COL with strength, extent, and positioning very comparable with their counterparts in CTR. Inspection of these fields at other levels, as well as the evolution of $[Z_{300}]$ and $[T_{500}]$ (Figs. 13 and 14), reveal also a good agreement among the simulations until 11 March 2005. Thus, it is suggested that the presence of the Andes cordillera or the occurrence of moist processes (within the domain) have little, if any, influence on the COL formation and intensification. Rather, the cyclone segregation from the extratropical trough and its subsequent intensification appear mostly driven by the large-scale, upper-level circulation as described in section 4, and only indirectly affected by the Andes cordillera though their impact on the hemispheric flow.

One might ask whether the similarities of the COL structure during its development arise, at least partially,

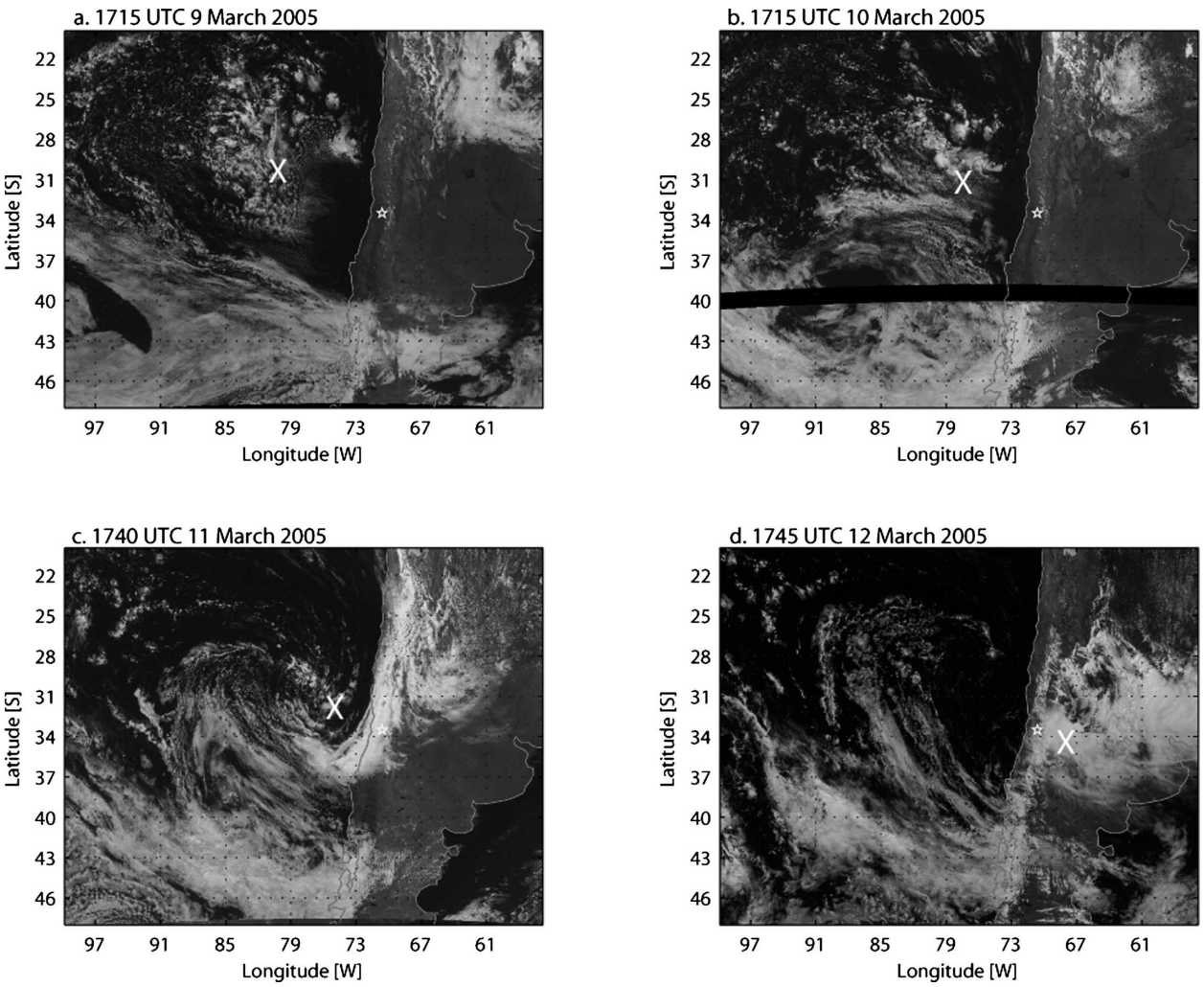

FIG. 9. *GOES-12* visible images over southwestern South America during the COL life cycle: (a) 1715 UTC 9 Mar 2005, (b) 1715 UTC 10 Mar 2005, (c) 1740 UTC 11 Mar 2005, and (d) 1715 UTC 12 Mar 2005. The cross indicates COL's center as derived from reanalysis data.

from the identical forcing imposed by the nearby west boundary. (There are also identical initial conditions but they probably have little effect after 3 days of integration.) Recall that these boundary conditions are taken from the NCEP–NCAR reanalysis, so they "feel" the presence of the Andes. To answer this question, we performed the ED and the EDNT experiments, where the western boundary was placed at 140°W, and so the impact of the lateral forcing on the COL genesis region should be smaller than in CTR. Again, the COL develops with or without topography, with similar structure and intensity in both simulations (not shown), supporting our claim that the Andes does not play a direct role on the COL genesis.

The second time shown in Fig. 12 (0600 UTC 12 March 2005, right panels) is representative of the COL demise. In all simulations, the COL is near the Andes, the geopotential height at its center has increased (COL is filling up) and the attending midlevel cold air pool has reduced with respect to the conditions 36 h before. The decay of the COL in Dry is, however, less marked than in CTR. This differential evolution is also evident on Fig. 13. In CTR, for instance, temperatures colder than −15°C at 500 hPa disappear early on 13 March 2005 right over the Andes. In Dry, air with temperature colder than −15°C did cross the Andes and, consistently, the low values of geopotential at the COL center persisted longer than in CTR. As shown in the previous section, advection (horizontal + vertical) did not produce a significant temperature change at the COL's center, so latent heat released by deep convection is the only process capable of producing the

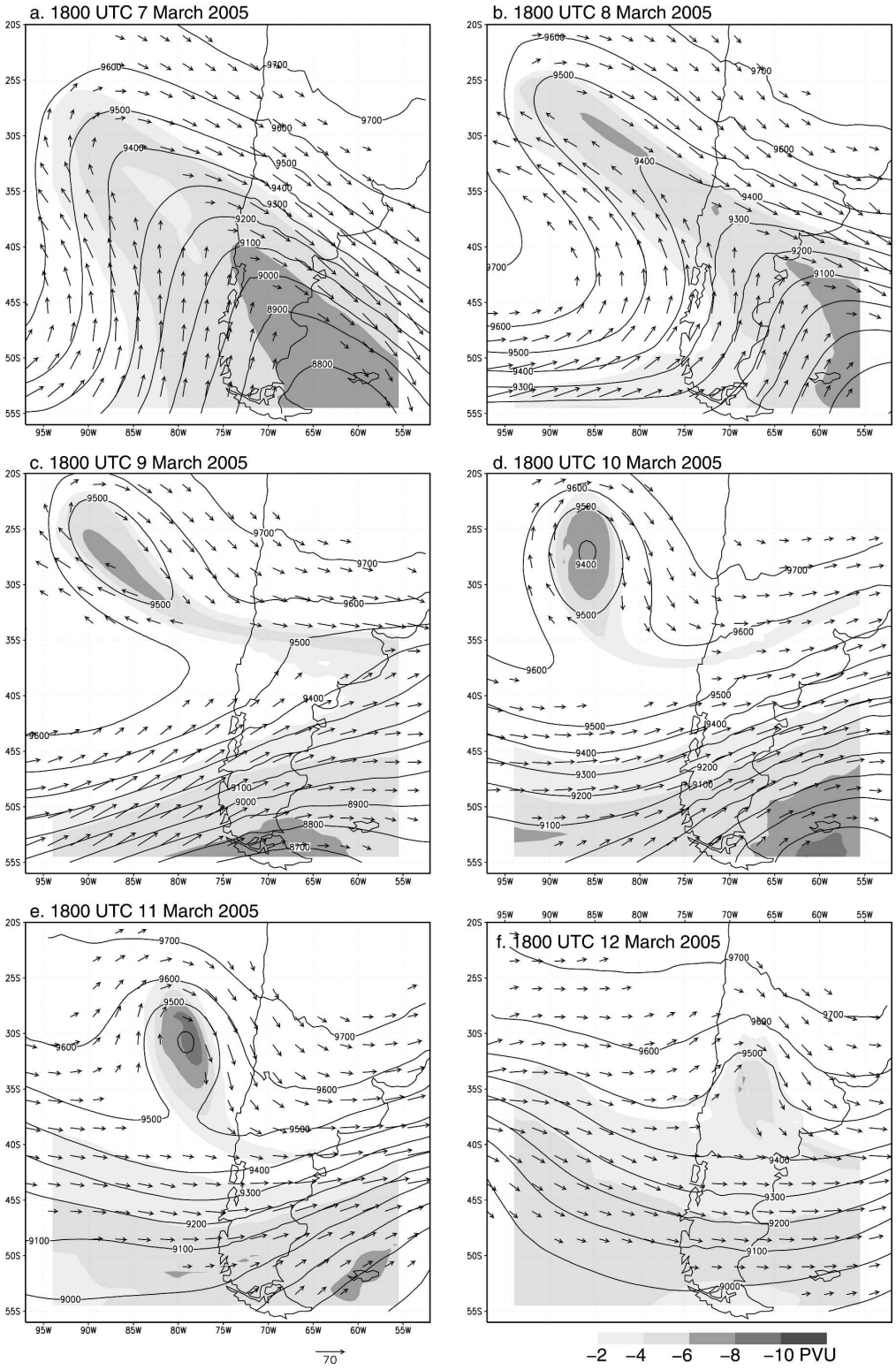

FIG. 10. Model geopotential height (CI 100 m) and wind vectors (scale at the bottom) at 300 hPa and potential vorticity at 340 K (shaded, scale at the bottom) at 1800 UTC (a)–(f) from 7 to 12 Mar 2005 (date and time indicated at the top). Wind vectors are not shown where wind speed is less than 20 m s^{-1}.

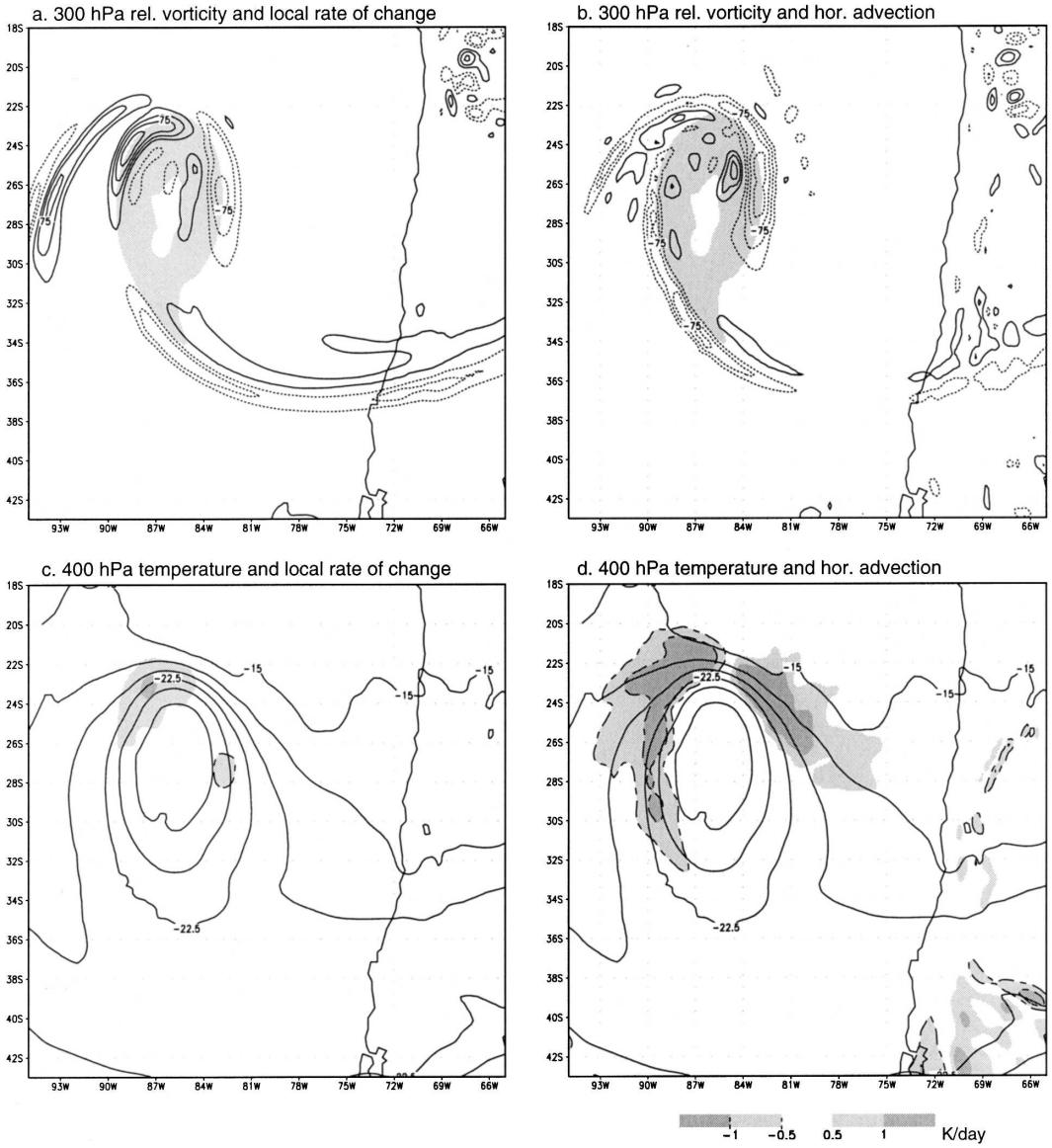

FIG. 11. (a) Local rate change of relative vorticity at 300 hPa (contours) at 1800 UTC 10 Mar 2005. The CI is 25 ($\times 10^{-10}$ s^{-2}), the negative values are in the dashed line, and the zero contour is omitted. The shaded area indicates negative relative vorticity larger than 20 ($\times 10^{-5}$ s^{-1}). (b) Same as in (a) but for horizontal advection of relative vorticity at 300 hPa (contours). (c) 400-hPa air temperature (CI 2.5 K) and local rate of change of air temperature (shaded according to scale at bottom right) at 1800 UTC 10 Mar 2005. (d) Same as in (c) but for horizontal advection of air temperature (shaded).

marked warming during the decaying stage of the COL. The weakening of the COL in Dry is dynamically produced by the upper-level flow plus a possible effect of the surface friction over the Andean high terrain.

In RTopo, the COL decayed more rapidly than in CTR. For instance, temperatures colder than −15°C at 500 hPa disappear 12 h before than the same condition in CTR and 500 km to the west of the Andes (Fig. 14). Figure 15a shows Q_C and T_{500} when the COL center was ~500 km away from the Andes for CTR. As described before (cf. Fig. 7), deep, high water content clouds are just found over the mountains. The same figure for RTopo (Fig. 15b) and the longitude–time section of Q_C (Fig. 14c) reveal that deep convection along the eastern flank of the COL appears 12 h before than in CTR, when the COL was still well away from the Andes. Thus, the earlier onset of convection in RTopo with respect to CTR seems to explain the more rapid midlevel warming and COL lysis in the former case. Trajectory analysis using RTopo (and EDNT) results

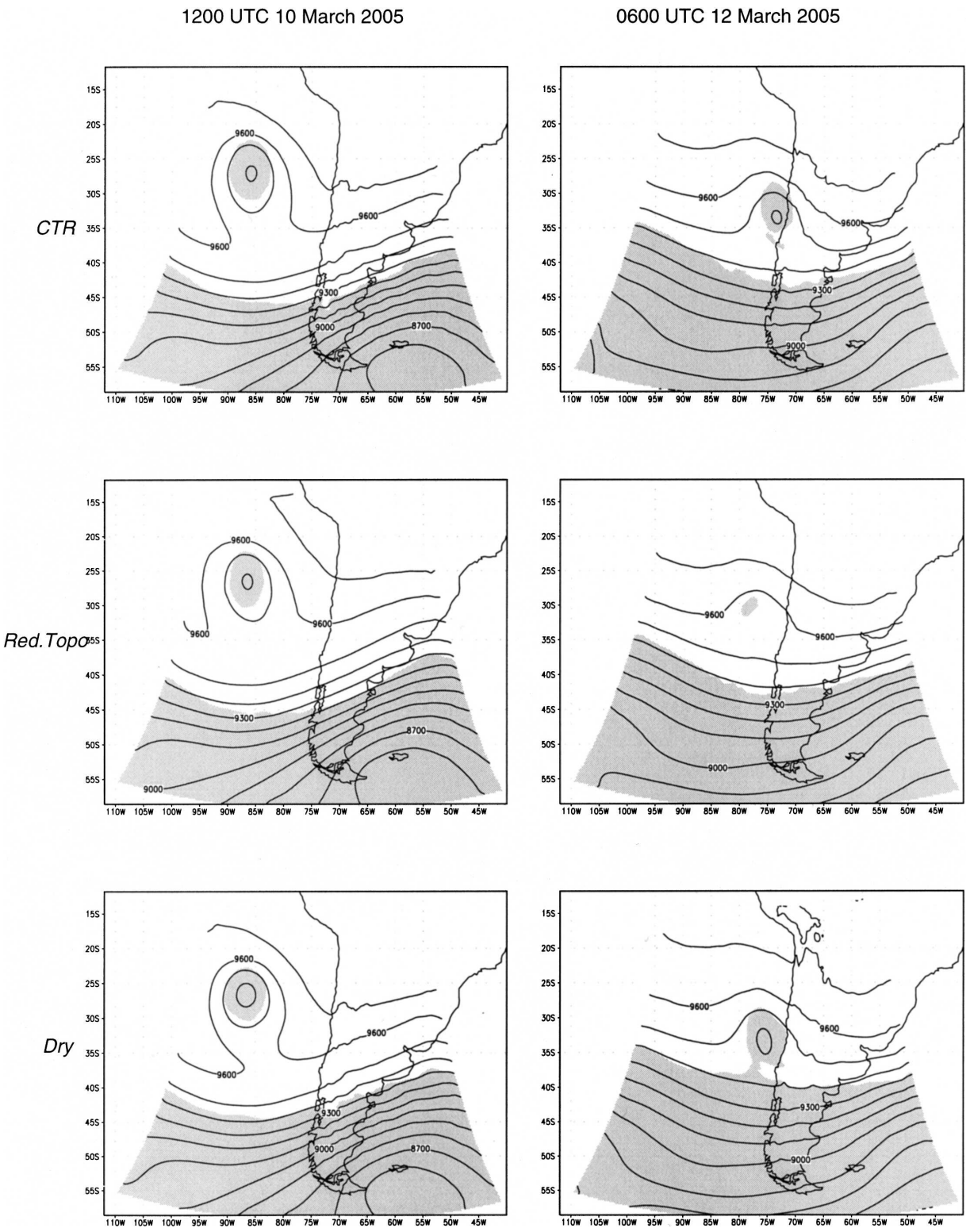

FIG. 12. Model geopotential height (CI 100 m) at 300 hPa and air temperature at 500 hPa (shaded indicates temperature below −15°C) at (left) 1200 UTC 10 Mar 2005 and (right) 0600 UTC 12 Mar 2005, from the (top) CTR, (middle) RTopo, and (bottom) Dry simulations.

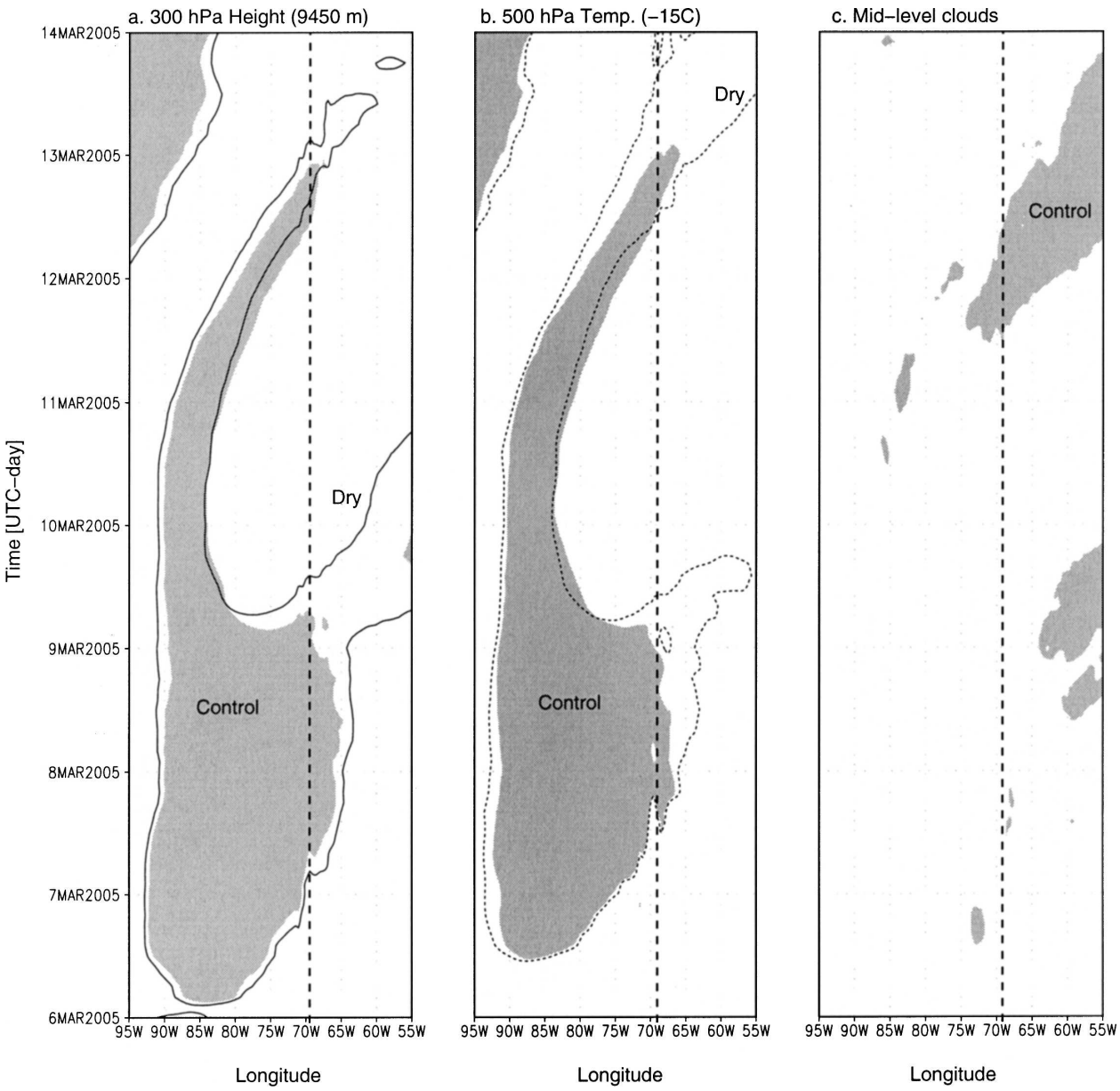

FIG. 13. (a) Time–longitude diagram of 300-hPa geopotential height averaged between 28° and 32°S. Shaded area indicates values less than 9450 m obtained in the CTR simulation. The contour outlines values less than 9450 m obtained in the Dry simulation. Vertical dashed line indicates the Andes ridge. (b) Same as in (a) but for air temperature at 500 hPa. The threshold in this case is −15°C. (c) Same as in (a) but for cloud mixing ratio averaged between 600 and 300 hPa. The threshold in this case is 2 ($\times 10^{-5}$ g kg^{-1}). There are no contours in this case because the Dry simulation does not have clouds.

reveal that even when the COL was over the Pacific, deep clouds form ahead of the COL fed by warm, humid air parcels ($\theta_e > 295$ K, not shown) drawn from the lower troposphere over the interior of the continent (Fig. 15b). In CTR, the presence of the Andes blocks any potential influx of continental air that could feed deep convection. Instead, in CTR, trajectories arriving to the region of strong ascending motion in the COL eastern flank originated at about 800 hPa over the Pacific (Fig. 15a), where cool, dry air prevails ($\theta_e < 280$ K, not shown).

6. Concluding remarks

The WRF model was used to simulate a typical COL that developed over the subtropical southeast Pacific on the second week in March 2005, and drifted eastward until it crossed the Andes cordillera where it de-

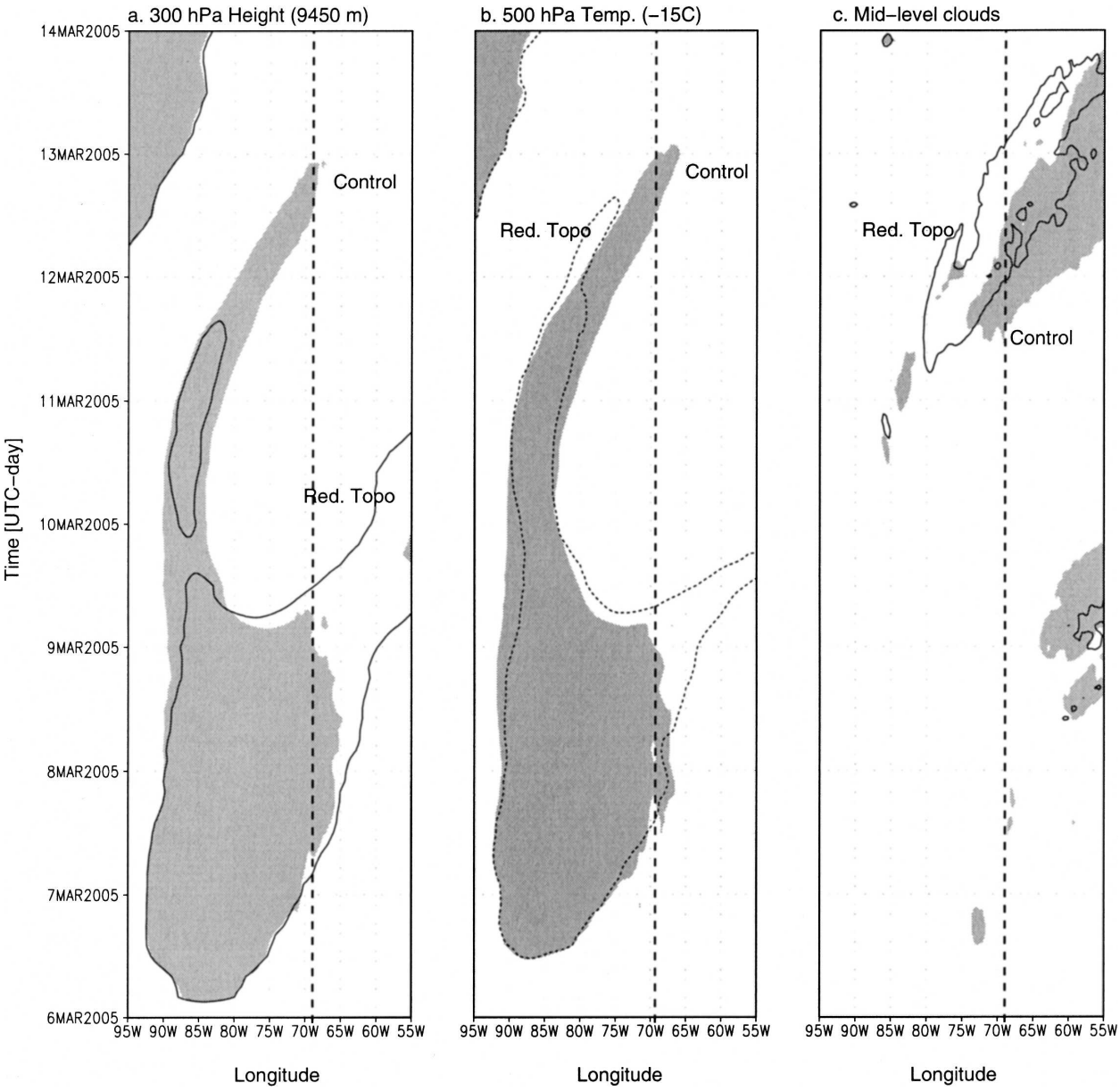

FIG. 14. Same as in Fig. 13, but the contour outlines results from the RTopo experiment.

cayed rapidly and produced moderate but unseasonal rainfall. The model was able to simulate the large-scale flow during the episode. The COL itself had a subsynoptic scale (hundreds of kilometers), and the model results compare favorably against limited upper-air, surface, and satellite observations during this episode.

The COL formed in a mid- and upper-level pressure pattern characterized by a trough extending from the southern tip of South America (midlatitudes) well into the subtropical southeast Pacific, and an upstream, quasi-stationary ridge reaching up to 50°S. Strong southwest flow (forming an acute angle with the trough axis) downstream of the ridge produced strong anticyclonic vorticity advection into the base of the trough, as well as horizontal warm advection that acted in concert with subsidence to warm that region. Downstream of the trough, the northwest winds were also strong but blowing more parallel to the trough axis, and consistently negative advection of vorticity and temperature were weak. Thus, the initial asymmetry in the wind direction around the parent trough seems key in the cyclone segregation, because it strangles the northwest–southeast-elongated cold trough at midlatitudes near the coastline.

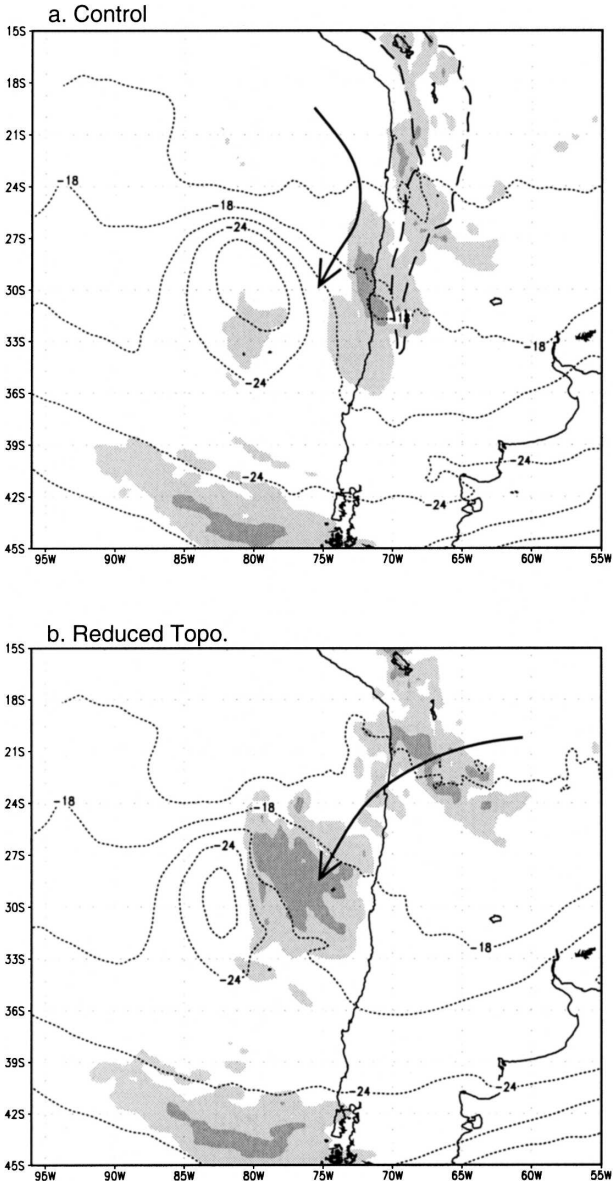

FIG. 15. (a) 400-hPa air temperature (CI 3°C) and cloud mixing ratio integrated between 600 and 300 hPa (light shading > 1 ($\times 10^{-5}$ g kg^{-1}), dark shading > 0 ($\times 10^{-5}$ g kg^{-1}) at 1800 UTC 11 Mar 2005 in CTR. The long-dashed line outlines terrain elevation in excess of 3000 m ASL. The solid arrow indicates 12-h backward trajectory of air parcels that arrive to the position of the arrowhead/800 hPa at 1800 UTC 11 Mar 2005. (b) Same as in (a) but for the RTopo experiment.

Once the COL formed, it drifted eastward driven mostly by vorticity advection. Vertical motion concentrated in the COL periphery, with subsidence (indirect circulation) upstream and ascent (direct circulation) downstream of the COL major axis. When the system was over the ocean, temperature changes were modest because the vertical and horizontal advection tended to cancel each other out, and diabatic heating was small in absence of significant clouds. The jet streak around the COL had an evolution similar to that observed in a classical wave as described in Keyser and Shapiro (1986), migrating from upstream of the inflection point to downstream.

To gauge the importance of the Andes cordillera and moist processes on the COL evolution, four sensitivity experiments were carried out: reduced topography, suppressed hydrometeors (Dry), extended domain, and no-topography over an extended domain. In all of them, the COL formed and exhibited similar position, strength, and extent as in the control simulation. Thus, the presence of the Andes cordillera or the occurrence of moist processes (within the domain) have little, if any, influence on the COL formation and intensification. Rather, the cyclone segregation appears mostly driven by the large-scale, upper-level circulation. The COL demise in the Dry simulation was much weaker than in the control, indicative of the primary role that diabatic heating by water vapor condensation plays on the COL dissipation. Such release of latent heat takes place in the deep, precipitating clouds that form over the Andes cordillera when the COL began to draw warm, moist air from the continent. Before that, air parcels ascending on the COL's eastern flank originate in the cool, dry environment over the eastern Pacific.

Thus, the Andes cordillera delays the COL demise by blocking the inflow of warm, moist air from the interior of the continent that would otherwise initiate deep convection. This "protective" effect of the Andes could explain, at least partially, the maximum frequency of COLs observed over the subtropical southeast Pacific (e.g., Fuenzalida et al. 2005), and might be generally applicable to other regions with similar geographic settings where a COL frequency maximum also verify: the subtropical southeast Atlantic (bounded by the South African plateau) and the subtropical northeast Pacific (bounded by the Rocky Mountains).

Acknowledgments. We thank Mark Falvey for his help in working with WRF and Rodrigo Sanchez for maintaining the Linux Cluster on which WRF was run. The authors are also grateful to Ricardo Muñoz, Patricio Aceituno, and two anonymous reviewers whose suggestions made possible significant improvements to this work. This work was supported by the Comisión Nacional de Investigación Científica y Tecnológica (CONICYT, Chile) under Project 1030757.

REFERENCES

Bell, G. D., and L. F. Bosart, 1993: A case study diagnosis of the formation of an upper-level cutoff cyclonic circulation over the eastern United States. *Mon. Wea. Rev.,* **121,** 1635–1655.

——, and D. Keyser, 1993: Shear and curvature vorticity and potential-vorticity interchanges: Interpretation and application to a cutoff cyclone episode. *Mon. Wea. Rev.,* **121,** 76–102.

Blackadar, A. K., 1979: High resolution models of the planetary boundary layer. *Advances in Environmental Science and Engineering,* J. R. Plaffin and E. Ziegler, Eds., Vol. 1, Gordon and Breach, 50–85.

Fuenzalida, H. A., R. Sanchez, and R. D. Garreaud, 2005: A climatology of cutoff lows in the Southern Hemisphere. *J. Geophys. Res.,* **110,** D18101, doi:10.129/2005JD005934.

Gayno, G. A., 1994: Development of a higher-order, fog-producing boundary layer model suitable for use in numerical weather prediction. M.S. thesis, Dept. of Meteorology, The Pennsylvania State University, 104 pp. [Available from Dept. of Meteorology, The Pennsylvania State University, University Park, PA 16802.]

Hong, S.-Y., J. Dudhia, and S.-H. Chen, 2004: A revised approach to ice microphysical processes for the bulk parameterization of cloud precipitation. *Mon. Wea. Rev.,* **132,** 103–120.

Hoskins, B. J., and K. I. Hodges, 2005: A new perspective on Southern Hemisphere storm tracks. *J. Climate,* **18,** 4108–4129.

——, M. E. McIntyre, and A. W. Robertson, 1985: On the use and significance of isentropic potential vorticity maps. *Quart. J. Roy. Meteor. Soc.,* **111,** 470, 877–946.

Kain, J. S., and J. M. Fritsch, 1993: Convective parameterization for mesoscale models: The Kain–Fritsch scheme. *The Representation of Cumulus Convection in Numerical Models, Meteor. Monogr.,* No. 24, Amer. Meteor. Soc., 165–170.

Kalnay, E., and Coauthors, 1996: The NCEP/NCAR 40-Year Reanalysis Project. *Bull. Amer. Meteor. Soc.,* **77,** 437–471.

Kentarchos, A. S., and T. D. Davies, 1998: A climatology of cutoff lows at 200 hPa in the Northern Hemisphere, 1990–1994. *Int. J. Climatol.,* **18,** 379–390.

——, G. J. Roelofs, and J. Lelieveld, 2000: Simulation of extratropical synoptic-scale stratosphere–troposphere exchange using a coupled chemistry GCM: Sensitivity to horizontal resolution. *J. Atmos. Sci.,* **57,** 2824–2838.

Keyser, D., and M. A. Shapiro, 1986: A review of the structure and dynamics of upper level frontal zones. *Mon. Wea. Rev.,* **114,** 452–499.

McInnes, K. L., and G. D. Hess, 1992: Modification to the Australian region limited area model and their impact on an east coast low event. *Aust. Meteor. Mag.,* **40,** 21–31.

Miky-Funatsu, B., M. A. Gan, and E. Caetano, 2004: A case study of orograghic cyclogenesis over South America. *Atmosfera,* **17,** 91–113.

Mishra, S. K., V. B. Rao, and M. A. Gan, 2001: Structure and evolution of the large-scale flow and an embedded upper tropospheric cyclonic vortex over northeast Brazil. *Mon. Wea. Rev.,* **129,** 1673–1688.

Nieto, R., and Coauthors, 2005: Climatological features of cutoff low systems in the Northern Hemisphere. *J. Climate,* **18,** 3085–3103.

Palmén, E., 1949: On the origin and structure of high-level cyclones south of the maximum westerlies. *Tellus,* **1,** 22–25.

Pizarro, J. G., and A. Montecinos, 2000: Cutoff cyclones off the subtropical coast of Chile. Preprints, *Sixth Int. Conf. on Southern Hemisphere Meteorology and Oceanography,* Santiago, Chile, Amer. Meteor. Soc., 301–303

Price, J. D., and G. Vaughan, 1993: The potential for stratosphere-troposphere exchanges in cut-off low systems. *Quart. J. Roy. Meteor. Soc.,* **119,** 345–365.

Rondanelli, R., L. Gallardo, and R. D. Garreaud, 2002: Rapid changes in ozone mixing ratios at Cerro Tololo (30°10′S, 70°48′W, 2200 m) in connection with cut-off lows and deep troughs. *J. Geophys. Res.,* **107,** 4201, doi:10.29/2001JD001334.

Skamarock, W. C., J. B. Klemp, J. Dudhia, D. Gill, D. Barker, W. Wang, and J. G. Powers, 2005: A description of the advanced research WRF version 2. NCAR Tech. Note TN-468+STR, 88 pp.

Smith, B. A., L. F. Bosart, D. Keyser, and D. St. Jean, 2002: A global 500 hPa cutoff cyclone climatology: 1953–1999. Preprints, *19th Conf. on Weather Analysis and Forecasting,* San Antonio, TX, Amer. Meteor. Soc., CD-ROM, P1.14.

Vuille, M., and C. Ammann, 1997: Regional snowfall patterns in the high, arid Andes. *Climatic Change,* **36,** 413–423.